Amalgamation of Photostriction, Photodomain, and Photopolarization effect in $BaTiO_3$ and its electronic origin

Anita Bagri[1], Anupam Jana[1], Gyanendra Panchal[1,2], Deodatta Moreshwar Phase[1] and Ram Janay Choudhary[1]*

[1] UGC-DAE Consortium for Scientific Research, Indore-452001, India

[2] Department Methods for Characterization of Transport Phenomena in Energy Materials, Helmholtz-Zentrum Berlin für Materialien und Energie, Berlin-14109, Germany

*Corresponding author: ram@csr.res.in

Keywords: Photostriction, Ferroelectric domains, Domain reorientation, Photopolarization, Electronic structure

Abstract

Multifunctional oxides offer huge potential for technological applications owing to their inclusive physical properties such as ferroelectricity, piezoelectricity, and electro-caloric. The natural occurrence of piezoelectricity, a tunable bandgap of ferroelectrics, opens a path to study the light-material interaction, leading to photoconduction and photovoltaic effects. Such light-controlled based devices yield additional advantages of weight reduction, wireless, and remote-controlled functionality over the heavy electric circuitry, hence, projected as an alternative solution to the traditional piezoelectric-based devices. Among these materials, lead-free $BaTiO_3$-based ferroelectric materials are a good choice for their potential applications with recently discovered light-controlled functionality. However, until now the coupling of light with the chemistry of ferroelectricity of the $BaTiO_3$ crystal has been elusive, although the ferroelectricity and piezoelectricity are well studied. Here, the present study reports the photostrictive effect of the order of 10^{-4} in the dimension of the *c*-domains of the tetragonal-$BaTiO_3$ crystal and domain reorientation at room temperature under the unpolarized, coherent visible-light illumination, consequently enhancement in polarization. The electronic origin of domain evolution and photostriction is explained by the light-induced modification in Ti 3*d*-O 2*p* hybridized orbitals. This facilitates the perspective of combining mechanical, electrical, optical, and functionalities in future generations of remotely controlled devices.

Introduction

The coupling of ferroelectric material with light is currently attracting interest due to its tremendous applications in photovoltaic devices. Besides the photovoltaic, the photostriction effect (non-thermal changes in the lattice dimension) is another interesting product of the coupling between light and ferroelectric properties, which has generated huge interest in recent years.[1-3] The natural occurrence of piezoelectricity in ferroelectrics plays a crucial role in the transformation of optical energy to mechanical strain and offers a huge prospect in wireless optomechanical applications, such as light-controlled elastic micromotors, microactuators, sensors, solar energy harvesting units, photoacoustic devices, etc.[4-8] Such optomechanical devices yield additional advantages of weight reduction, wireless, and remote-controlled functionality and therefore, are projected as an alternative solution to the traditional piezoelectric or magnetostrictive based electromechanical units.

$BaTiO_3$ (BTO) is a classic lead-free ferroelectric material with a significantly higher piezoelectric constant ($d_{33} \approx 85.6$ pC.N^{-1}) at room temperature (RT) [9-10] and hence may reveal better prospects for the photostrictive effect. Paillard and Yang *et al.* [11-12] theoretically investigated the opto-ferroelastic behavior of BTO (*R3m* symmetry) and found that the pseudo-cubic lattice constant of BTO shrinks upon increasing the number of photoexcited electrons. Rubio-Marcos *et al*. showed the reversible photoresponses of BTO single crystal under the polarized, coherent visible light illumination, such as photo-strain, domain wall motion, switching, and macroscopic changes in polarization.[4,13-14] Owing to the large bandgap of BTO, the possibility of the photovoltaic effect was discarded for such photo-induced effects in these reported studies. [4,13-14] Besides this, recently, the role of bulk photovoltaic effect as well as the light polarization in the optical control of domain configuration, is reported.[15] BTO crystal exhibits alternating

arrangement of in-plane polarized *a*-domains and out-of-plane polarized *c*-domains at RT with head-to-head (H-H) and tail-to-tail (T-T) configuration of polarization. It is reported that the *a*/*c* domain wall (at H-H configuration, appearing at the ridge) is under the larger stress as compared to the *c*/*a* domain wall (T-T configuration, appearing at the trough) due to the large accumulation of the charges.[16-19] It was revealed microscopically that the direction of polarization of incident light mainly affects the 90° domain wall, which leads to the domain wall motion. Under the illumination, this accumulation of the charges is responsible for the origin of *b* domains, interestingly only in the *c*-domain region at the *a*-*c* domain wall, to release the accumulated stress.[13-14] In BTO crystal, it was observed that under the light illumination, *c* and *b*-domains evolve at the cost of *a*-domains irrespective of the dominance of the domain in the crystal.[13-14] These evidences suggest that in BTO single crystal the polarization direction of domains plays key factor for the photosensitivity of these domains and hence probed by using the angle dependence of polarized light.[15] However, the previous studies are utterly limited to the optical control of domain-configuration utilizing the in-plane polarization of incident light, where a necessary question in poly-domain configuration systems remains unanswered *why only the certain polarized state of domains, primarily the out-of-plane polarized domains (c-domains) and adjacent domain wall in BTO, is more photosensitive as compared to the in-plane polarized domains even under the unpolarized light?*

In this study, we present conclusive proof of the origin of photostriction in the *c*-domain of $BaTiO_3$ single crystal. The higher surface energy of the *c*-domains becomes a cause of the preferential location for water absorption and responsible for higher sensitivity towards the photoresponse, which can be switched by illumination even with unpolarized visible light. The electronic origin of domain evolution and photostriction is explained by the light-induced

modification in Ti 3*d*-O 2*p* hybridized orbitals and demonstrated by polarized x-ray absorption spectroscopy (*p*XAS). The observed relative photostriction in the out-of-plane lattice parameter of the *c*-domain is found to be of the order of 10^{-4}. Moreover, 12% *a* to *c*-domain switching is observed under the illumination. Consequently, the polarization along the ferroelectric axis of the *c*-domain is enhanced by 40% at RT. The present study explicitly reveals conjointly interacting among different facets such as structure, domains, polarization, light, mechanical distortion with strong applicative potential in oxide-based future electronics.

Results and Discussion

Light-induced changes in the crystal structure of $BaTiO_3$ single crystal. The basic identification of the structure and crystalline orientation of the single crystal was performed using x-ray diffraction (XRD). Additional material and structural details are provided in Supporting Information S1. The θ/2θ XRD patterns of BTO crystal recorded with and without the visible light-illumination (532 nm and 633 nm) depict the (002) and (200/020) Bragg reflections of *c*-domains and *a*-domains respectively (**Figure 1**a, b)**.** XRD patterns reveal the higher relative intensity of the *a*-domains than the *c*-domains, suggesting the dominance of the *a*-domains in the studied BTO single crystal. Under the light illumination, (002) orientation, the peak corresponding to *c*-domains shifts towards the higher 2θ value, which accounts for the photo-strain (ε_λ), estimated by ε_λ (%) $= \left(\frac{L_\lambda - L_{Dark}}{L_{Dark}}\right) \times 100$, where, L_{Dark} and L_λ are the lattice parameters in the dark and under the illumination condition respectively, and found to be compressive of 0.07% (**Table 1**). Interestingly, the peak corresponding to *a*-domains, (200/020) orientation does not show any observable deviation. Also, the full width at half maxima (FWHM) of these peaks is found to be decreased with the illumination, more details of light-induced changes in the XRD peaks are

provided in Supporting Information S2. Besides this, the ratio of integrated intensities ($I_{max}.B$, where I_{max} is the maximum intensity and B is FWHM) of *c*-domains to *a*-domains ($R = I_c / I_a$) enhances from $R_{Dark} = 0.036$ to $R_{Light} = 0.049$ for 532 nm and 0.053 for 633 nm, suggesting the enhanced fraction of *c*-domains, at the cost of *a*-domains, *i.e.* 90° domain reorientation. The percentage of 90° domain reorientation N ; [$N = \{(R_{Dark} - R_{Light}) / (R_{Dark} + 2\ R_{Light})\}\times 100$] is estimated to be 9.7 and 11.9% for 532 and 633 nm respectively, similar to the earlier report, which suggests the switching of 7.5%.[14] The observed enhancement in the intensity of the *c*-domains is akin to the electric field effect on BTO substrate applied perpendicular to its plane, which also mimics similar variation in intensity, i.e., I_c / I_a ratio.[20-21] We shall like to emphasize here that the observed photo-domain effect does not arise due to local temperature changes upon the light illumination, since in that scenario, contrary to our observation, (i) the intensity of diffraction peaks should decrease, and (ii) FWHM B should increase.[22] Besides, earlier it is reported that the intensity ratio I_c / I_a remains constant in ferroelectric BTO with enhanced temperature, as well as both the (002) and (200/020) peak positions shift in the opposite direction.[21] The possibility of domain coalescence is also ruled out since the diffuse scattering (S_D) between (002) and (200) degenerated reflections remain unaltered (Figure 1a,b), which is directly related to the domain wall fraction of the material.[23] We also observe that the system retains its original structural parameters after eight hours of light illumination, which gives strong evidence of optical memory storage properties of BTO single crystal.

Photopolarization effect in BTO single crystal. To probe the consequences of the observed photostriction and photo-domain effect on the ferroelectric properties of BTO single crystal, we have performed the polarization versus electric field (P-E) measurement in the presence of light-illumination with the applied electric field direction being along the out-of-plane (*c*-axis) of the

BTO crystal at RT. Figure 1c, d depicts the enhanced polarization along the *c*-direction of BTO crystal, under the illumination of 532 nm and 633 nm light respectively. The maximum enhancement is observed at remanent polarization P_r, defined by the photo-polarization effect ΔP_r %, $[\Delta P_r\% = (\frac{P_r^{light} - P_r^{Dark}}{P_r^{Dark}}) \times 100]$ is found to be as high as ~ 40%, which manifests that light excitation can be an alternative to the electric field to tune the remanent polarization state. It transpires that the combination of light with the electric field eases the reorientation of the domains along the polar axis of the *c*-domains. Here, one can argue that the origin such changes in the P-E loop can be arise due to the photocurrent via photovoltaic effect. Therefore, we have also estimated the contribution in the polarization changes owing to the photovolatic effect, considering the photocurrent of the order of 10^{-11} A[15]. The changes in the polarization owing to this photocurrent are found to be five times lesser order than the changes we observed in the P-E loop under the light illumination. Therefore, such a negligible contributions from the photovolaic effects are omitted as a cause of polarization changes under the light illumination.

Light-induced modification in the electronic structure of BTO single crystal. It is known that the Ti 3*d*-O 2*p* hybridization is responsible for the ferroelectric instability in the BTO system.[24] Thus the observed photo-strain, photo-domain, and photo-polarization effects must arise from the modification in Ti 3*d*-O 2*p* orbital hybridization strength with light-illumination. To probe the electronic origin, we have recorded the RT *p*XAS in the absence and presence of visible light (532 nm and 633 nm) at O *K* and Ti *L*-edge as shown in **Figure 2** and **Figure 3** respectively. In the absorption process for O *K*-edge, an electron undergoes a transition from the oxygen 1*s* orbital to unoccupied states of oxygen-metal hybridized *p*-*d* orbitals and hence provides the information related to the covalent mixing of metal and oxygen orbitals, whereas, Ti *L*-edge is very much sensitive to the subtle variation in the local environment at the Ti-site. Features A and B in O *K*-

edge (Figure 2) arise due to hybridized states between O-2*p* and Ti 3*d* t_{2g} and 3*d* e_g respectively, which are separated by the TiO_6 octahedral ligand field splitting (Δ_{CF}), and further split due to the tetragonal distortion [Schematic I]. Feature C is attributed to O-2*p* derived states hybridized with Ba-5*d* orbitals.[25] The O *K*-edge spectra have been recorded in $E||c$ and $E\perp c$ configurations of x-ray polarization with and without the illumination of 532 nm and 633 nm light. In the present study, we considered all the in-plane polarized domains as *a*-domain. Since the absorption spectra are not domain-specific, therefore, the spectra recorded at $E\perp c$ will have the dominant contribution of in-plane orbitals of *a* and *c*-domain, whereas, $E||c$ will have the dominant contribution of out-of-plane orbitals contributions in the absorption spectra. Accordingly, as illustrated in Schematic II, at $E\perp c$ condition, either d_z^2 or $d_{x^2-y^2}$ or both of the orbitals of *a*-domains and $d_{x^2-y^2}$ of *c*-domains predominantly contributes to the Ti 3*d* e_g -O 2*p* overlapped intensity, while at $E\|c$, $d_{x^2-y^2}$ of *a*-domain and d_z^2 of *c*-domains contributes dominantly. For $E||c$, O *K*-edge spectra (Figure 2a, b) reveal that with the light illumination, feature B (Ti 3*d* e_g -O 2*p*) shifts marginally towards the lower photon energy side and becomes narrower. A careful observation of feature B of O *K*-edge spectra in the dark state suggests that this feature comprises of two shoulders B1 (at lower photon energy side) and B2 (at higher photon energy side). Since the tetragonal structure of BTO has a larger *c* lattice parameter than *a* or *b*, the Coulombic interaction energy for d_z^2 will be lower than that $d_{x^2-y^2}$ [Schematic I]. Therefore, the lower energy feature B1 should represent the d_z^2 states of the *c*-domains, while the higher energy feature B2 should represent the $d_{x^2-y^2}$ states of the *a*-domains.

Under the illumination condition, the narrowing of feature B suggests the reduced energy difference in the Coulombic repulsion energy for the abovementioned orbitals. This is possible only when the tetragonal structure system tends to the higher symmetry configuration upon light

illumination. It is evident that feature B1 enhances with the illumination, whereas feature B2 diminishes. Since the probing area of the sample is not changed under the illumination, therefore, the change in the intensity of B1 is not solely related to the enhanced hybridization of O 2*p*-Ti 3 d_z^2 of *c*-domains, (in that scenario the Δ_{CF} would increase) rather it is also related to the enhanced *c*-domain fraction under the light illumination. The decreased intensity of feature B2 reflects the decreased contribution of *a*-domains in feature B. The average peak position of feature B shifts towards the lower photon energy side due to the intensity variation of B1 and B2. The increased relative intensity of features B1/B2 is reflecting the domain reorientation of the fraction of *a*-domains to *c*-domains under the light illumination, consistent with the XRD findings. The intensity of feature C is also observed to be decreased slightly, suggesting the reduced overlap of Ba 5*d*-O 2*p* orbitals due to a change in the tetragonality under the light illumination.

At normal incidence ($E \perp c$) also (Figure 2c, d) under the light illumination condition, it is observed that feature A remains unchanged, however, the intensity of feature B is slightly increased, whereas the intensity of feature C is slightly decreased. These observations suggest the modification in the axial overlap of Ti 3*d*-O 2*p* and Ba 5*d*-O 2*p* orbitals under the light illumination, causing structural modification as well as change in the polarization distortion.

Figure 3a,b, and 3c,d depicts the Ti *L*3-edge spectra, taken at $E \| c$ and $E \perp c$ configurations respectively under the illumination of 532 and 633 nm light. Ti *L*3-edge reveals two features L_A and L_B arise due to the octahedral crystal field splitting, corresponding to Ti 3*d* t_{2g} and Ti 3*d* e_g states at lower and higher energy positions respectively. With the illumination of light, for the E||*c* case, feature L_B slightly shifts towards a lower photon energy value. Feature L_B is comprised of two features corresponding to the Ti $3d_z^2$ (L_{B1}) of *c*-domains (at lower photon energy side) and $3d_{x^2-y^2}$ (L_{B2}) state of *a*-domains (at the higher photon energy side). The detailed variation in these

features of Ti $L3$ edge under the light illumination is described in Supporting Information S3. The narrowing of feature L_B is related to a decrease in the energy gap between the d_z^2 or $d_{x^2-y^2}$ states of e_g derived band. The enhanced intensity ratio of L_{B1}/ L_{B2} is concomitant with the O K-edge observations of domain reorientation. For $E \perp c$, we do not observe any noticeable change in the Ti L edge.

Discussion.

In previous studies, the role of photovoltaic effect for the photo-domain or photo-strain effects owing to the large bandgap of BTO is under debate.[4, 13-14] It is known that the BTO surface layer consists of the stable chemisorbed and physisorbed humid species.[26] He *et al*.[27] revealed that 95% of humid water droplets choose *c*- domains as the preferential adsorption location to nucleate. The AFM image of the studied BTO crystal, as shown in **Figure 4** also suggests that the *c*-domain and the adjacent domain wall of crystal are fully humidified, whereas the *a* domain of the crystal does not show the water droplet coverage. The presence of water droplets on the BTO crystal surface is also confirmed by x-ray photoemission measurements, discribed in Supporting Information S4, which reveal the feature corresponding to water adsorption at higher binding energy position in O 1s core-level spectra, as also reflected from the AFM micrograph. The detail investigation of these AFM micrographs are provided in the supporting infromation S5. Since the *c*- domains are polarized either upward (c^+) or downward (c^-) direction with respect to the *a*-*b* plane of crystal, the induced charges on the surface lead to the higher surface and electrostatic energy as compared to the *a*-domains. Polar H_2O molecules prefer to absorb on the *c*-domain to neutralize the surface charge, whereas the *a*-domain has no surface charges.[28-30] The chemisorbed water droplets create sub-bandgap states leading to the inarticulate bandgap energy values reported in the literature from 1.81 eV to 3.4 eV in its ferroelectric ground state.[31-36] The existence of sub-bandgap states allows

the absorption of visible light by the *c*-domains of BTO dominantly as shown in the Supporting Information S6, hence the photo-voltaic effect. Whereas, *a*-domains show lesser sensitivity to the visible light illumination. Thus, the *c*-domains of the BTO crystal is more responsible for the observed changes in the various properties upon light illumination as compared to the *a*-domain.

The P-E study reveals the maximum photo-polarization at remanence state 40 % with the 0.07 % out-of-plane compressive photo-induced strain and 12 % *a* to *c*-domain switching. Earlier the cause of reversible change in domain rearrangement was attributed to the light-driven domain wall motion. The accumulated charges at the domain wall create an asymmetric saw-teeth potential,[37-39] leading to the so-called ratchet effect, which causes the domain wall motion.[40-41] In our study, under the light illumination, besides the emergence of *b*-domain, which is confirmed by Raman measurements, discribed in the Supporting Information S7. It is also observed that the photo-induced effects take few hours to relax, in contrast to reversible nature, Therefore, the origin of these effects in the present study is not solely linked with the reversible domain wall motion. As discussed above, the photovoltaic effect can not be discarded, particularly for *c*-domains. The photoferroelectric phenomena in BTO crystal is associated with the extreme filling of traps and domain boundaries by the localized carriers and recharging of these traps with the illumination by the visible light. Photoejected charge carriers enhance the charge concentration at the surface of the crystal, which decreases the screening length. Consequently, the redistribution of electric fields and charges occur inside the crystal. The increase of field in crystal volume accelerates the nucleation of domains and the system gets its minimum energy with the process of polydomainization via domain reorientation. Accordingly, the studied BTO single crystal, which contains the majority of *a*-domains, undergoes the *c*-domainization with the light-illumination, as confirmed from the XRD pattern under the illumination. The redistribution of electric fields also

causes the converse piezoelectric effect in $BaTiO_3$ leading to the observed 0.07% photo-compressive strain in the *c*-domain. It should be noted here that the corresponding photo-strain energy can also be partially accountable for the observed photo-domain effect. The photodomainization also leads to the enhanced polarization of the crystal. A careful observation of the P-E loop also reveals notable irreversibility in the P-E loop, since the chemisorbed water droplets create a local strain field, which is responsible for the irreversible domain wall motion.

It is known that in the non-centrosymmetric BTO ferroelectric, polarization is caused due to shifting of the cation (Ti^{4+}) and the anions (O^{2-}) in opposite directions along the c-axis about the Ba positions.[42] In the tetragonal BTO crystal, owing to the *P*4*mm* symmetry of both *a*- and *c*-domains, the electronic structure of both the domains will be same, however in the present study owing to the presence of water droplets at the *c*-domains, the electronic structure of *c*-domains will be modified and different from the *a*-domains. Under the light illumination, owing to the larger photovolatic effects in *c*-domains owing to the subbandgap states created by the chemi and physi-absorbed water droplets shows the predominent changes in the electronic structure of *c*-domains. Here, we want to mention that owing to the P4*mm* symmetry of both *a*- and *c*-domains, the unpolarized light illumination differ the both domains based on the strength of the photovoltaic effects rather based on the polar axis direction. In the overall study, it is observed that as compared to Ti 3*d* e_g -O 2*p* overlap, Ti 3*d* t_{2g} - O 2*p* overlap does not reveal noticeable variation upon light illumination, possibly owing to smaller separation between the tetragonally splitted t_{2g} orbitals due to relatively weaker π bonding. Besides, Song *et al.*[43] have shown that in BTO, Ti e_g orbitals are more responsible for the change in *c/a* ratio than the t_{2g} orbitals. It is also quite evident from the E|| *c* O *K*-edge study, under the illumination, such that the Ti 3*d* d_z^2-O 2*p* hybridization of the *c*-domain dominates over $d_{x^2-y^2}$-O 2*p* of *a*-domain, reflecting the domain reorientation from *a* to *c*-

domain as observed in the XRD measurement. The narrowing of the e_g derived band in the O *K*-edge as well as in Ti *L*3 edge reflects the reduced energy difference between the Ti 3*d* d_z^2-O 2*p* and $d_{x^2-y^2}$-O 2*p*, hybridized states, concomitant with the structural changes towards higher symmetry configuration with the light illumination. Under the light illumination, it was observed earlier[15] that the photoresponse of the Ba-O bond depends upon the domain type and was dominant for *a*-domain as compared to the *c*-domain. Under the light illumination, the significant domain reorientation from *a*-domain to *c*-domain can modify this contribution, leading to the reduced intensity of Ba 5*d* -O 2*p* overlap hybridized states. All the observations are reproducible *e.g.* the XAS spectra, recorded with and without the light illumination, are shown in Supporting Information S8. Indeed, the visible light illumination changes in the *c*-lattice parameter of *c*-domain, intensity of *c*-domain, Ti 3*d* e_g -O 2*p* and Ba 5*d*-O 2*p* hybridization, which give rise to modification in the ferroelectric properties.

Conclusion

To summarize, here we report the photostrictive properties and photo domain effect in ferroelectric BTO crystal. The *c*-domain of $BaTiO_3$ compresses along the polar axis under the illumination with visible light and relative compression of 10^{-4} is observed. The illumination modulates the kinetics of the domain wall motion. The *a* to *c*-domain switching of 12% is observed with the visible light-illumination. The enhanced fraction of *c*-domains leads to the enhancement in the polarization along the (*00l*) direction. These observations are accounted for the domain wall motion as well as the converse piezoelectric effect. A careful observation of the trend of Ti 3*d* –O 2*p* orbitals overlap in the presence of light illumination suggests that the intensity ratio of the d_z^2 states of *c*- domain to the $d_{x^2-y^2}$ states of the *a*- domain increases with the light illumination. The present study

explicitly reveals conjointly interacting different facets such as structure, domains, polarization, light, mechanical distortion of an otherwise robust d^0- ferroelectrics. This opens the new way for potential applications in several types of wireless devices and sensors, light-controlled elastic micromotors, microactuators, and other interesting optomechanical systems.

▪ Associated Content

EXPERIMENTAL SECTION

Sample details: High quality commercial $BaTiO_3$ (BTO) single crystal (4 mm × 4 mm × 0.5 mm) was used for the study (supplied by Crystal GmbH). No additional chemical and thermal treatments were employed to reveal the domain structure.

X-ray diffraction measurement: X-ray diffraction (XRD) measurements were carried out using a Bruker D2 PHASER setup with Cu K_α lab source (λ=1.5406 Å), collecting data in θ/2θ geometry. At room temperature, it is well known that the BTO exhibits the tetragonal (*P*4*mm*) phase containing *a*-domain (*l00/0l0*) and *c*-domain (*00l*) with the ferroelectric ground state. In the present study, we considered all in-plane polarized domains as *a*-domain (*l00/0l0*) and all out-of-plane polarized domains as *c*-domain (*00l*). At humid environment, water droplets easily grow on the BTO surface. To do the experiment in the illumination condition, we have used the unpolarized coherent visible laser diode with the wavelength of 532 nm and 633 nm and of the power of 40 mW for illumination, whereas the data collected during the off condition of light illumination is considered as the dark condition. The light spot was adjusted at 1.0 mm diameter using the iris.

Polarized X-ray absorption spectroscopy: To investigate the electronic origin of photoresponses, we have performed the room temperature polarized x-ray absorption spectroscopic (*p*XAS) measurements at O *K*-edge (520-550 eV) and Ti *L* – edge (450-470 eV) in total electron yield (TEY) mode under 10^{-8} Torr vacuum at polarized light soft X-ray absorption beamline at RRCAT, Indore, India. To collect the data in different polarization configurations, we have tilted the sample about the incident beam direction. For E ⊥ *c* configurations, the surface normal of the BTO crystal is made parallel to the incident beam direction, whereas in E || *c* configurations, the angle between the direction of beam propagation and surface normal is kept at 75°. During the *p*XAS measurement after the illumination light, another dark state spectra is collected after eight hours. To illuminate the sample, laser diode of 532 and 633 nm with 40 mW power were used. The spot size of incident beam is 0.5 mm diameter in our XAS measurements, which is much greater than the domain size, present in the studied crystal of BTO. The energy resolution during the XAS measurements is better than 0.25 eV at room temperature for the O *K* and Ti *L*-edge energy range.

Atomic force microscopic measurements: An atomic force microscope (AFM) was used to collect the topographic information of the domain structure at the surface of the single crystal. AFM measurements were performed by the Bruker Biscope Resolve set up with Silicon Nitride tip (Si_3N_4), in the contact mode configuration.

Polarization versus electric field (P-E) measurement: P-E measurements were performed using the Precision Materials Analyser, Radiant Technologies. Inc. Thin layer of silver paste was coated on both sides of the BTO sample. Two metallic pins were connected to front and back electrodes

via mechanical contact. To do the experiment under the illumination conditions, a laser diode of 532 and 633 nm with 40 mW power were used.

SUPPORTING INFORMATION

Supporting Information is available free of charge on ACS Publications website or from the author.

AUTHOR INFORMATION

Corresponding Authors

Ram Janay Choudhary- UGC-DAE Consortium for Scientific Research, Indore-452001, India; https://orcid.org/0000-0003-0029-1541 E-mail: ram@csr.res.in

Authors

Anita Bagri - UGC-DAE Consortium for Scientific Research, Indore-452001, India; https://orcid.org/0000-0003-1427-7054

Anupam Jana - UGC-DAE Consortium for Scientific Research, Indore-452001, India; https://orcid.org/0000-0002-2967-9315

Gyanendra Panchal – Department Methods for Characterization of Transport Phenomena in Energy Materials, Helmholtz-Zentrum Berlin für Materialien und Energie, Berlin-14109, Germany; https://orcid.org/0000-0001-5208-8831

Deodatta Moreshwar Phase- UGC-DAE Consortium for Scientific Research, Indore-452001, India; https://orcid.org/0000-0002-0185-0686

Author Contributions

A.B. and R.J.C. conceived the concept and course of problem; A.B., A.J. and G.P. planned the experiments with the assistance of R.J.C. A.B. collected the XRD, PE, XAS and AFM data. A.B, A.J. and G.P. analyzed the XRD, PE, XAS, and AFM data with the assistance of R.J.C. and D.M.P. A.B. wrote the manuscript along with R.J.C., using the substantive feedback from A.J. and G.P.

ACKNOWLEDGMENTS

We thank Dr.V.G. Sathe and A. K. Rathore for Raman measurements, Dr. R.Venkatesh and M. K. Gangrade for AFM measurements, Dr.V. R. Reddy for the optical micrograph with polarized light, and Dr. Ram Prakash for Diffuse reflectance measurements. A.B. is also thankful to A.Wadikar and R. Sah for helping in the *p*XAS measuments. A.B. is highly grateful to Dr. R. Rajamani, Dr. R. Rawat, Rishabh Shukla, and Akash Surmapalli for fruitful discussions.

CONFLICT OF INTEREST

The authors declare no conflict of interest.

REFERENCES

[1] Paillard, C.; Bai, X.; Infante, I.C.; Guennou, M.; Geneste, G.; Alexe, M.; Kreisel, J.; Dkhil B. Photovoltaics with Ferroelectrics: Current Status and Beyond. *Adv. Mater.* **2016**, 28, 5153-5168.

[2] Chen, C.; Yi, Z. Photostrictive Effect: Characterization Techniques, Materials, and Applications. *Adv. Funct. Mater.* **2021**, 31, 2010706.

[3] Kundys, B. Photostrictive Materials. *Appl. Phys. Rev.* **2015**, 2, 011301.

[4] Rubio-Marcos, F.; Páez-Margarit, D.; Ochoa, D. A.; Del Campo, A.; Fernandez, J. F.; García, M. A. Photo-Controlled Ferroelectric-Based Nanoactuators. *ACS Appl. Mater. Interfaces* **2019**, 11, 13921-13926.

[5] Wang, J.; Ma, J.; Yang, Y.; Chen, M.; Zhang, J.; Ma, J.; Nan, C. W. Ferroelectric Photodetector with High Current on–off Ratio ($\sim 1\times10^4$%) in Self-Assembled Topological Nanoislands. *ACS Appl. Electron. Materials* **2019**, 1, 862-868.

[6] Palagi, S.; Singh, D.; Fischer, P. Light-Controlled Micromotors and Soft Microrobots. *Adv. Opt. Mater.* **2019**, 7, 1900370.

[7] Li, Y., Shi, R. An Intelligent Solar Energy-Harvesting System for Wireless Sensor Networks. *J Wireless Com Network* **2015**, 2015, 179.

[8] Uchino K. New Applications of Photostrictive Ferroics. Materials Research Innovations *Mater. Res. Inno*. **1997**, 1, 163-168.

[9] Berlincourt, D.; Jaffe, H.; Elastic and Piezoelectric Coefficients of Single-Crystal Barium Titanate. *Phys. Rev. B.* **1958**, 111, 143-148.

[10] Graf, M.; Sepliarsky, M.; Machado,R.; Stachiotti, M.G. Dielectric and Piezoelectric Properties of $BiFeO_3$ from Molecular Dynamics Simulations. *Sol. Stat. Comm.* **2015**, 218, 10-13.

[11] Paillard, C.; Prosandeev, S.; Bellaiche, L. *Ab initio* Approach to Photostriction in Classical Ferroelectric Materials. *Phys. Rev. B* **2017**, 96, 045205.

[12] Yang, Y.; Paillard, C.; Xu, B.; Bellaiche, L. Photostriction and Elasto-Optic Response in Multiferroics and Ferroelectrics from First Principles. *Jour. of Phys.: Cond. Matt.* **2018**, 30, 073001.

[13] Rubio-Marcos, F.; Del Campo, A.; Marchet, P.; Fernandez, J. F.´ Ferroelectric Domain Wall Motion Induced by Polarized Light. *Nat. Commun*. **2015**, 6, 6594.

[14] Rubio-Marcos, F.; Ochoa, D. A.; Del Campo, A.; García, M. A.; Castro, G. R.; Fernandez, J. F.; García, J. E. Reversible Optical Control of Macroscopic Polarization in Ferroelectrics. *Nat. Photonics* **2018** 12, 29-32.

[15] Dwij, V.; De, B. K.; Rana, S.; Kunwar, H. S.; Yadav, S.; Sahu, S.R.; Venkatesh, R.; Lalla, N. P.; Phase, D. M.; Shukla, D. K.; Sathe, V. G. Optical control of Domain Configuration through Light Polarization in Ferroelectric $BaTiO_3$. *Phys. Rev. B* **2022**, 105, 134103

[16] Rubio-Marcos, F.; Del Campo, A.; Ordoñez-Pimentel, J.; Venet, M.; Rojas-Hernandez, R.E.; Páez-Margarit, D.; Ochoa, D.A.; Fernández, J.F.; García, J.E. Photo controlled Strain in

Polycrystalline Ferroelectrics via Domain Engineering Strategy. *ACS Appl. Mater. Interfaces* **2021,** 13, 20858-20864.

[17] Mokry, P.; Tagantsev, A. K.; Fousek, J. Pressure on Charged Domain Walls and Additional Imprint Mechanism in Ferroelectrics. *Phys. Rev. B: Condens. Matter Mater. Phys*. **2018**, 75, 094110.

[18] Sluka, T.; Tagantsev, A. K.; Bednyakov, P.; Setter, N. Free Electron Gas at Charged Domain Walls in Insulating $BaTiO_3$. *Nat. Commun*.**2013,** 4, 1808.

[19] Bednyakov, P. S.; Sluka, T.; Tagantsev, A. K.; Damjanovic, D.; Setter, N. Formation of Charged Ferroelectric Domain Walls with Controlled Periodicity. *Sci. Rep*. **2015**, 5, 15819.

[20] Valot, C. M.; Berar, J.F.; Courtois, C.; Mesnier, M. T.; Niepce, J.C.; Maglione, M. X-Ray Diffraction Diagram Evolution of a $BaTiO_3$ Ceramic under an Electric Field. *Ferro. Lett. Sec.* **1994**, 17, 5-12.

[21] C. M. Valot, C. M.; Floquet, N.; Perriat,P.; Mesnier, M.; Niepce, J.C. Ferroelectric Domains in $BaTiO_3$, Powders and Ceramics Evidenced by X-Ray Diffraction. *Ferroelectrics* **1995**, 172, 235-241.

[22] Cullity, B. D. *Elements of X-ray Diffraction*, **1978**.

[23] Ghosh, D.; Sakata, A.; Carter, J.; Thomas, P.A.; Han, H.; Nino, J.C.; Jones J.L. Domain Wall Displacement is the Origin of Superior Permittivity and Piezoelectricity in $BaTiO_3$ at Intermediate Grain Sizes. *Adv. Opt. Mater.* **2014**, 24, 885896.

[24] Cohen, E. R.; Krakauer, H. Electronic Structure Studies of the Differences in Ferroelectric Behavior of $BaTiO_3$ and $PbTiO_3$, *Ferroelectrics* **1992,** 136, 65-83.

[25] Panchal, G.; Shukla, D. K.; Choudhary, R. J.; Reddy, V. R.; Phase, D. M. The Effect of Oxygen Stoichiometry at the Interface of Epitaxial $BaTiO_3/La_{0.7}Sr_{0.3}MnO_3$ Bilayers on Its Electronic and Magnetic Properties. *J. Appl. Phys.* **2017**, 122,085310.

[26] Peter, F.; Szot, K.; Waser, R. Piezoresponse in the Light of Surface Adsorbates: Relevance of Defined Surface Conditions for Perovskite Materials. *Appl. Phys. Lett*. **2004**, 85, 2896.

[27] He, Y. D.; Qiao, L. J.; Volinsky, A. A.; Bai, Y.; Wu, M.; Chu, Y. W. Humidity Effects on (001) $BaTiO_3$ Single Crystal Surface Water Adsorption. *Appl. Phys. Lett.* **2011,** 98, 062905.

[28] He, D.Y.; Qiao, L. J.; Volinsky, A. A.; Bai, Y.; Guo, L.Q. Electric Field and Surface Charge Effects on Ferroelectric Domain Dynamics in $BaTiO_3$ Single Crystal. *Phys. Rev. B.* **2011**, 84, 024101.

[29] He, D.Y.; Qiao, L. J.; Volinsky, A.A. Humidity Effect on BaTiO3 *c-d*omain Surface Potential Inversion Induced by Electric Field. *J. Appl. Phys.* **2011**, 110, 074104.

[30] Jiang, B.; Bai, Y.; Chu, W. Y.; Shi, S. Q.; Qiao, L.J.; Su, Y. J. Effect of Humidity on Domain Switching Behaviors of $BaTiO_3$ Single Crystal under Sustained Load. *Appl. Surf. Sci.* **2008**, 254, 17, 5594-5598.

[31] Cox, G. A.; Roberts, G.; Tredgold, R. H.; The Optical Absorption Edge of Barium Titanate. *Brit. J. Appl. Phys.* **1966**, 17,743-745.

[32] Bhowmick, M.; Xi, H.; Ullrich, B. Optical Bandgap Definition via a Modified Form of Urbach's Rule. *Materials* **2021**, 14, 1639.

[33] O' Leary, S. K.; Zukotynski, S.; Perz, J. M. Semiclassical Density-of-States and Optical-Absorption Analysis of Amorphous Semiconductors. *Phys. Rev. B.* **1995**, 51, 7.

[34] Wang, J.; Xing, Z.; Lu, Z.; Ding, K.; Wang, H. First-Principle Study of the Properties in $BaTiO_3$ and the Electronic Structure of H_2O Adsorption on $BaTiO_3$. *Int. J. Quantum. Chem.* **2021**,121, e26576.

[35] Sanna, S.; Thierfelder, C.; Wippermann, S.; Sinha, T. P.; Schmidt, W. G.; Barium Titanate Ground- and Excited-State Properties from First-Principles Calculations. *Phys. Rev. B* **2011**, 83, 054112.

[36] Gupta, G.; Nautiyal, T.; Auluck, S. Optical Properties of the Compounds $BaTiO_3$ and $SrTiO_3$. *Phys. Rev. B* **2004**,69, 052101.

[37] Yang, S. Y.; Seidel, J.; Byrnes, S. J.; Shafer, P.; Yang, C.-H.; Rossell, M. D.; Yu, P.; Chu, Y.-H.; Scott, J. F.; Ager, J. W.; Martin, L.W.; Ramesh, R. Above Bandgap Voltages from Ferroelectric Photovoltaic Devices. *Nat. Nanotechnol.* **2010**, 5, 143-147.

[38] Seidel, J.; Fu, D.; Yang, S.Y.; Alarcon-Llado´, E.; Wu, J.;´ Ramesh, R.; Ager, J. W. Efficient Photovoltaic Current Generation at Ferroelectric Domain Walls. *Phys. Rev. Lett.* **2010**, 107, 126805 (2010).

[39] Liu, S.; Zheng, F.; Koocher, N. Z.; Takenaka, H.; Wang, F.; Rappe, A. M. Ferroelectric Domain Wall Induced Band Gap Reduction and Charge Separation in Organometal Halide Perovskites. *J. Phys. Chem. Lett.* **2015**, 6, 693-699.

[40] Perez-Junquera, A.; Marconi, V. I.; Kolton, A. B.; A´´varez-Prado, L. M.; Souche, Y.; Alija, A.; Velez, M.; Anguita, J. V.; Alameda, J. M.;´ Martín, J. I.; Parrondo, J. M. R. Crossed-Ratchet Effects for Magnetic Domain Wall Motion. *Phys. Rev. Lett.* **2008**, 100, 037203.

[41] Franken, J. H.; Swagten, H. J. M.; Koopmans, B. Shift Registers Based on Magnetic Domain Wall Ratchets with Perpendicular Anisotropy. *Nat. Nanotechnol.* **2012**, 7,499-503.

[42] Harada, J.; Pedersen, T.; Barnea, Z. X-Ray and Neutron Diffraction Study of Tetragonal Barium Titanate. *Acta Cryst.* **1970**, A26, 336.

[43] Song, Y.; Liu, X.; Wen, F.; Kareev, M.; Zhang, R.; Pei, Y.; Bi, J.; Shafer, P.; N'Diaye, A. T.; Arenholz, E.; Park, S. Y.; Cao, Y.; Chakhalian, J. Unconventional Crystal-field Splitting in Noncentrosymmetric $BaTiO_3$ Thin Films. *Phys. Rev. Materials* **2020**, 4, 024413.

Table 1. Quantification of photoresponses of BTO crystal: Calculated lattice parameters [± 0.001 Å] of $BaTiO_3$ single crystal in different conditions during XRD measurements (Dark and with the illumination of light of different wavelength) and corresponding photostrain ε_λ (where λ = 532 and 633 nm) and change in the polarization in the remanent state ($\Delta Pr\%$).

Table. 1:

Parameter	Dark	532 nm	ε_λ (%)	633 nm	ε_λ (%)
c	4.041 Å	4.038 Å	-0.07	4.038 Å	-0.07
a	3.999 Å	3.999 Å	0	3.999 Å	0
c/a	1.010	1.009	-	1.009	
ΔPr [%]	-	+23	-	+39.4	-

Figure captions:

Figure.1. Unequivocal evidence of optically induced structural changes in ferroelectric domains and its ferroelectric response at macroscopic scale: Magnified room temperature x-ray diffraction (XRD) patterns of (002) and (200/020) Bragg reflections of tetragonal $BaTiO_3$ single crystal with and without light illumination (a) 532 nm and (b) 633 nm. S_D indicates the diffuse scattering, related to the domain wall fraction. Room temperature polarization versus electric field (P-E) study of $BaTiO_3$ single crystal with and without light illumination (c) 532 nm and (d) 633 nm. In the diagram black, green and red colored pattern represents the data collected in three different condition dark, 532 and 633 nm light illumination respectively.

Schematic I. Rearrangement of Ti 3*d* orbitals of $BaTiO_3$ single crystal owing to the tetragonal distortion.

Schematic II. Schematic diagram of polarized x-ray absorption of poly-domain $BaTiO_3$ single crystal.

Figure.2. Dramatic photo response of Ti 3*d*-O 2*p* overlap: Polarized x-ray absorption spectra (*p*XAS) of $BaTiO_3$ single crystal at O *K*-edge with and without light illumination, (a) and (b) at E||*c* with 532 nm and 633 nm respectively, (c) and (d) at E⊥*c* with 532 nm and 633 nm respectively.

Figure.3. Light induced modification in the electronic structure of BTO: Polarized x-ray absorption spectra (*p*XAS) of $BaTiO_3$ single crystal at Ti *L*3 edge with and without light illumination, (a) and (b) at E||*c* with 532 nm and 633 nm respectively, (c) and (d) at E⊥*c* with 532 nm and 633 nm respectively.

Figure.4. Topographical image of the BTO crystal: (a) and (b) Atomic force Micrograph of $BaTiO_3$ single crystal of $60 \times 60\ \mu m^2$ dimension and its schematic.

Figure.1:

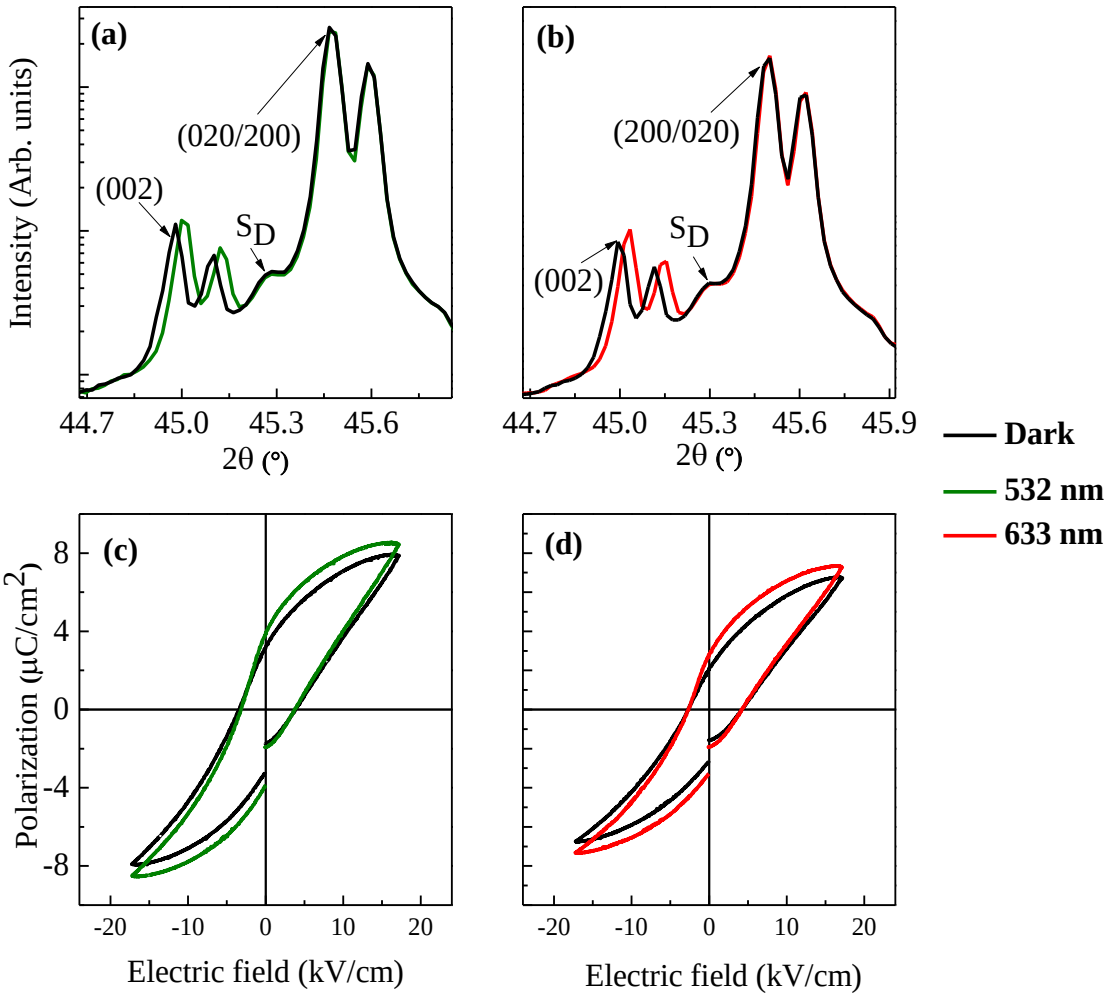
(a)
(020/200)
(002)
S_D
Intensity (Arb. units)
44.7
45.0
45.3
45.6
2θ (°)
(b)
(200/020)
(002)
S_D
44.7
45.0
45.3
45.6
45.9
2θ (°)
Dark
532 nm
633 nm
(c)
Polarization (μC/cm²)
8
4
0
-4
-8
-20
-10
0
10
20
Electric field (kV/cm)
(d)
-20
-10
0
10
20
Electric field (kV/cm)

Schematic I:

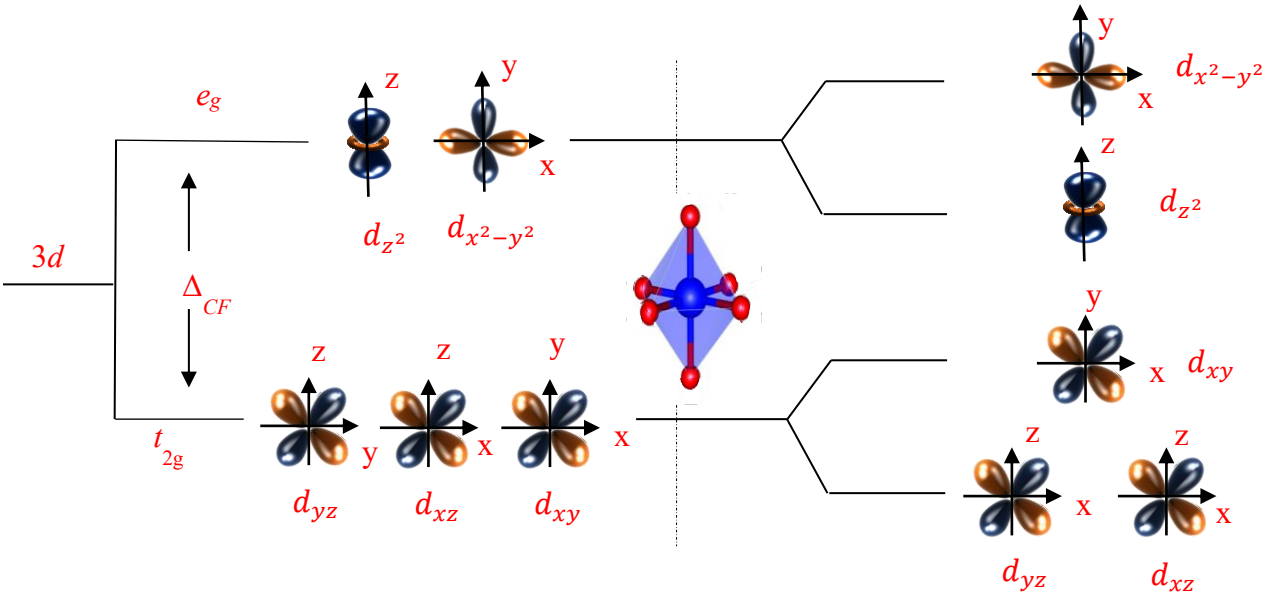

Schematic II:

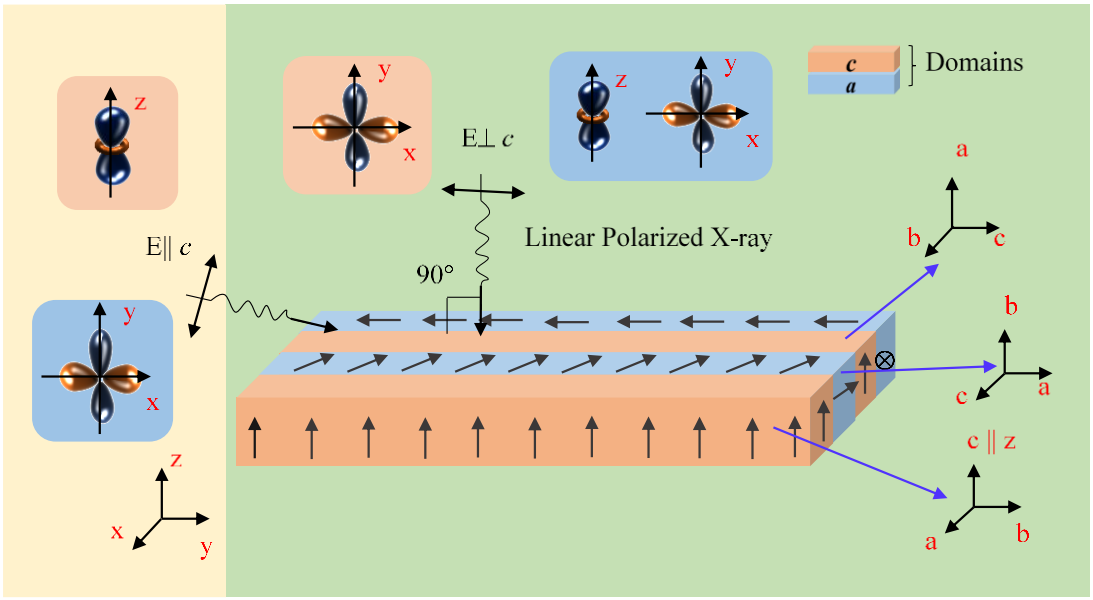

Figure. 2:

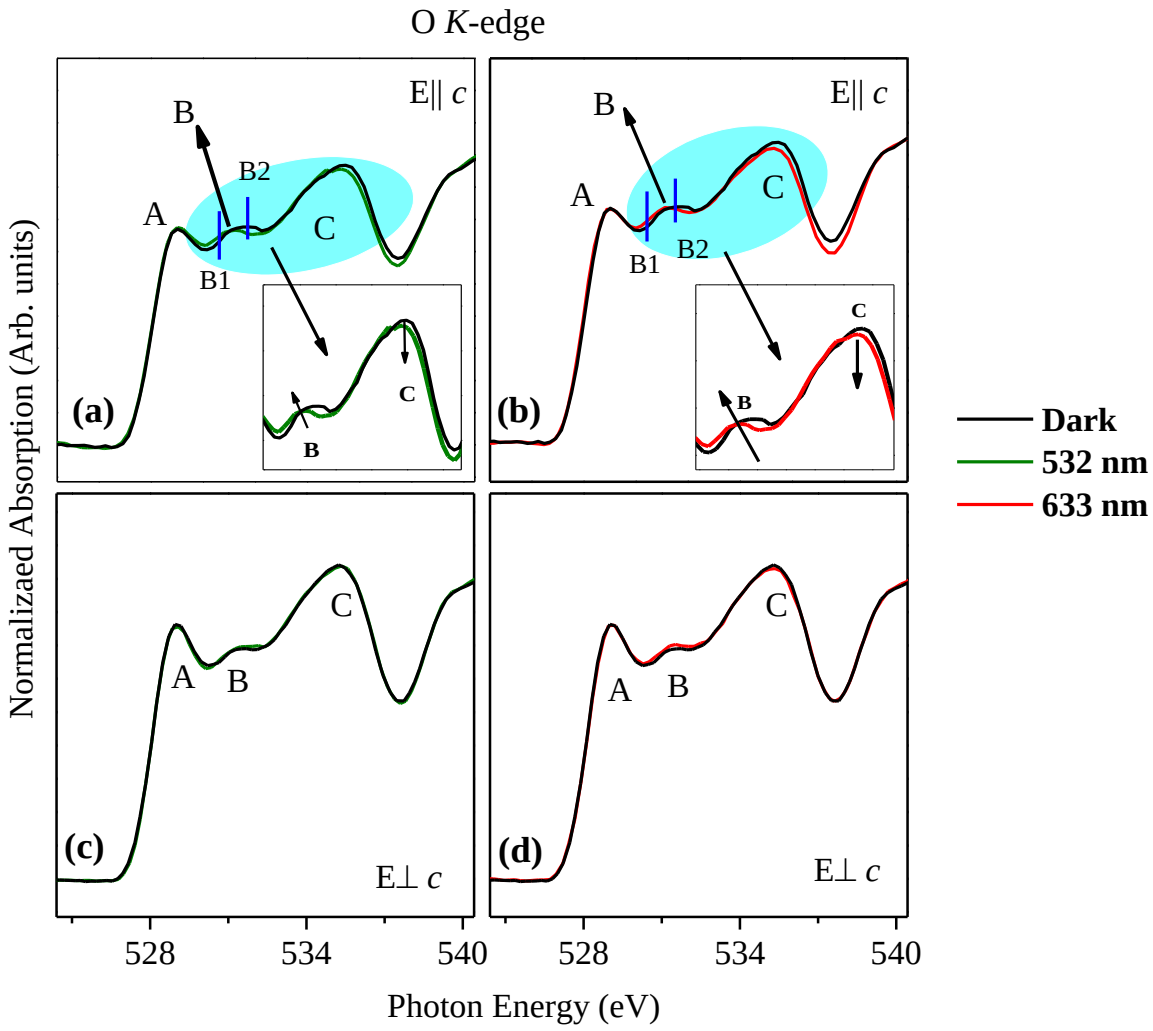
O K-edge
E|| c
B
B2
A
C
B1
(a)
(b)
E⊥ c
(c)
(d)
Normalizaed Absorption (Arb. units)
528
534
540
Photon Energy (eV)
Dark
532 nm
633 nm

Figure. 3:

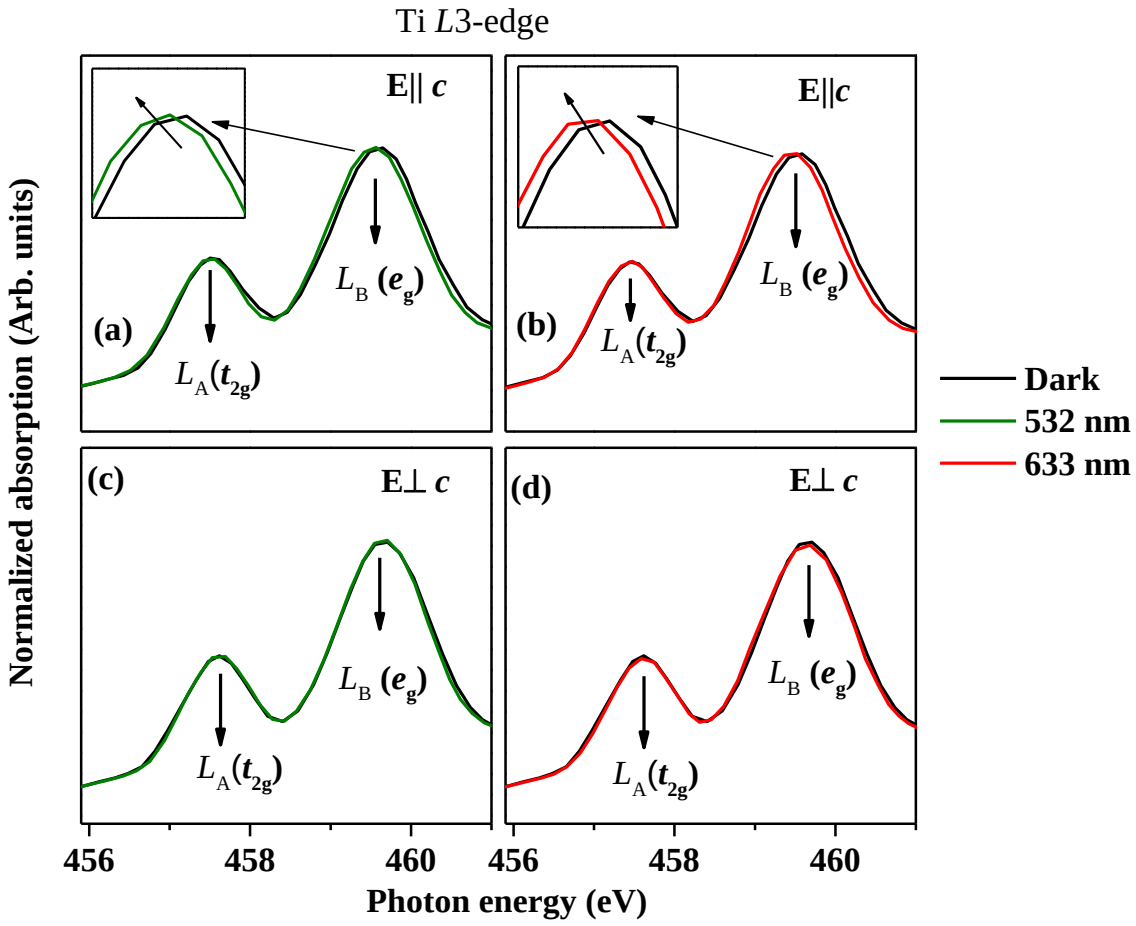
Ti L3-edge
E|| c
E||c
E⊥ c
E⊥ c
(a)
(b)
(c)
(d)
L_B (e_g)
L_A(t_{2g})
Normalized absorption (Arb. units)
Photon energy (eV)
456
458
460
Dark
532 nm
633 nm

Figure. 4:

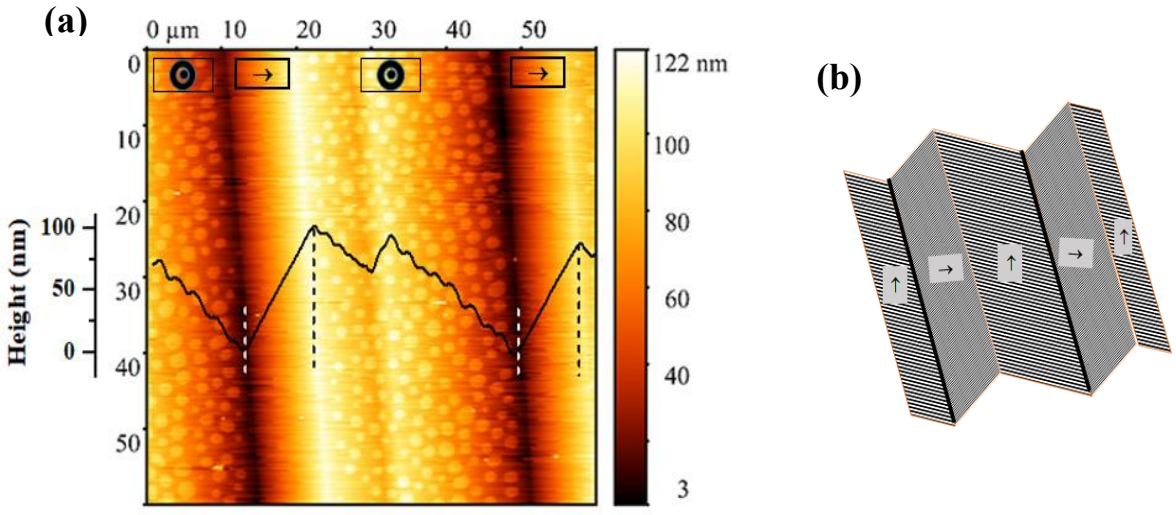
(a)
0 µm
10
20
30
40
50
0
10
20
30
40
50
Height (nm)
100
50
0
122 nm
100
80
60
40
3
(b)

Table of Contents

- A ***compressive photo strain is only observed in the c-domains*** of $BaTiO_3$ single crystal.
- In $BaTiO_3$ single crystal, ***a partial a to c-domain switching*** is observed with visible light illumination.
- Under the visible light illumination, the enhanced relative fraction of *c*-domains consequent to ***40 % enhancement in the polarization*** at room temperature.
- Under the visible light illumination, the ***electronic structure of c-domains is modified***.